Binding of thymine and Molybdenocene dichloride anticancer agent: A DFT investigation

Maryam Azari[1], Reza Ghiasi[2,*], Behrooz Mirza[1]

[1] Department of Chemistry, Karaj Branch, Islamic Azad University, Karaj, Iran
[2] Department of Chemistry, East Tehran Branch, Islamic Azad University, Tehran, Iran

ARTICLE INFO

ABSTRACT

This study investigated the reaction of molybdenocene dichloride complex (Cp_2MoCl_2) as anticancer agent with thymine using mPW1PW91 functional. Five possible modes of the binding of thymine to $MoCp_2^{2+}$ were considered. Energetic stability of five isomers was compared in gas and aqueous phases. Also, the solvent effect on the dipole moment values of systems was illustrated. The solvent effect on these data were examined using conductor polarizable continuum model (C-PCM). Energy decomposition analysis (EDA), Interaction region indicator (IRI) and Quantum theory of atoms in molecules (QTAIM) analysis provided deep insights into the nature and the strength of the Molybdenocene–thymine binding. Charge decomposition analysis (CDA) was used to illustrate the transfer of charge between two fragments.

1. Introduction

Metallocene dihalides and pseudo halides (Cp_2MX_2, Cp refer to cyclopentadienyl, M is Mo, Ti, Nb, V) possess biological propensity for a huge range of human and murine tumors [1-8]. It is well known in this regard that, Cp_2Ti^{2+} hydrolyzes extensively under physiological conditions, whereas Cp_2Mo^{2+} is hydrolytically stable [9, 10]. In this years have been prepared several thiol derivatives of molybdenocene and studies on cell uptake and cytotoxicity of them were pursued [11]. In a research, biological Interaction of Cp_2MoCl_2 with Bovine Serum Albumin Using Fluorescence Spectroscopy has been reported [12]. Interactions of nucleobases of DNA and RNA with metals [13-15] and anticancer drugs has been examined with computational methods [16-19]. For the reason that DNA is frequently the assumed target for metal-based drugs, various researches have dedicated on nucleobase interactions [20-22]. The aqueous nucleobase and nucleotide coordination chemistry of Cp_2MoCl_2 has been investigated [23]. In regard to the nucleobases, N-methylcytosine and N-methyladenine (to simulate the N-functionalized coordination environment in DNA, were used N-methylated nucleobases, were formed cyclic chelates of strained four-membered Mo(IV) with one amino proton deprotonation and concurrent coordination to both the amine (exo-) and heterocyclic (endocyclic) cytosine and adenine nitrogen atoms.

In the base of our knowledge., interaction of molybdenocene dichloride anticancer agent with thymine has been not studied. Therefore, we interested to illustration of computational study of the binding of this drug to thymine. Solvent impact on dipole moment values of the systems was illustrated. Interaction region indicator (IRI) and energy decomposition analysis (EDA) provided deep insights into the nature and the strength of the interaction. Charge decomposition analysis (CDA) was used to illustrate charge transfer among two fragments.

2. Computational Methods

For calculations the package of Gaussian 09 software was used [24]. For the main groups of elements standard 6-311G(d,p) basis set [25-28] was used, while the Def2-TZVPPD basis set was described for the Mo element [29]. To exclude correlation integrals related to 14

electrons of the Mo atom and direct calculation of the exchange, pseudo-potential effective core potential (ECP) was utilized on the Def2-TZVPPD basis set [30]. Optimization of the geometry was applied using the parameter hybrid functional with correlation (mPW1PW91) and adapted Perdew-Wang exchange was considered [31].

To demonstrate that the optimization structures don't have imaginary frequency, harmonic vibrational frequencies were done.

For the solvation impact study, a self-consistent reaction field (SCRF) approach was used in this paper through conductor-like polarizable continuum model (CPCM) [32, 33].

For illustration of the bonding interactions between the thymine… MoCp$_2$ energy decomposition analysis (EDA) was studied with Multiwfn 3.8 software package [34]. The interaction energy (ΔE_{int}) between the two fragments was evaluated as:

$$\Delta E_{int} = \Delta E_{polar} + \Delta E_{els} + \Delta E_{Ex}$$

Where ΔE_{polar} is the electron density polarization term (the induction term), ΔE_{els} is the electrostatic interaction and ΔE_{Ex}, as the exchange repulsion terms, respectively. Interaction region indicator (IRI) [35], Quantum theory of atoms in molecules (QTAIM) analysis and Charge decomposition analysis (CDA) [36] by Multiwfn 3.8

package were provided [34, 37]. VMD software was employed to the visualizations of the IRI graphs [38].

3. Results and discussion

3.1 Energetic aspects

Reaction of molybdenocene dichloride complex (Cp$_2$MoCl$_2$) as anticancer agent with thymine is considered as:

Cp$_2$MoCl$_2$ + thymine $\rightarrow$ Cp$_2$Mo…thymine + 2 Cl$^-$
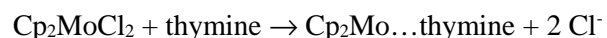
Five possible modes of the binding of thymine to MoCp$_2^{2+}$ are indicated. In Table 1, these complexes energy and relative energy values are listed. It can be found the trend of stability of these isomers is: **T5-O** > **T2-O** > **T1-N** > **T3-N** > **T4-C**. Therefore, the most stable isomer is **T5-O** isomer. Also, C-PCM calculations are done on these molecules by considering water as solvent. Computed energy and relative energy values are listed in Table 1. Energetic changing trends are identical in gas and aqueous phase. Hydration energy values of the isomer are calculated by the following equation:

$$\Delta E_{hydration} = E(Water) - E(gas)$$

It can be seen, $\Delta E_{hydration}$ values increase as:

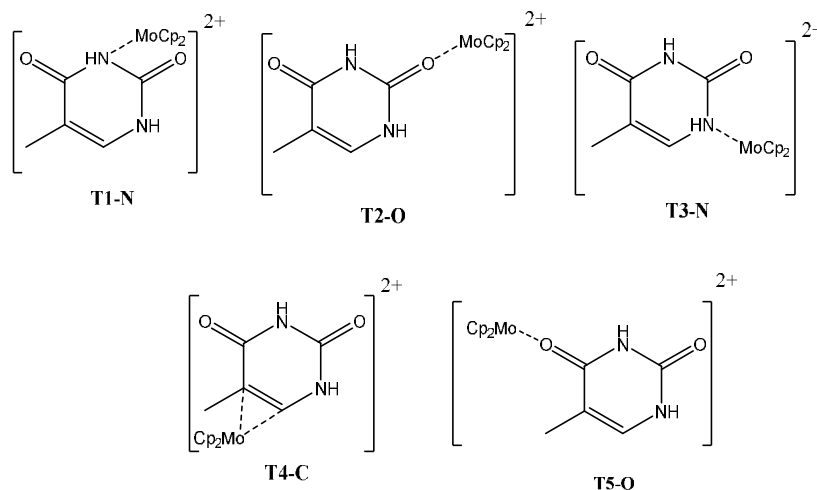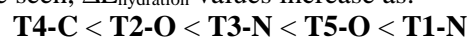**T4-C** < **T2-O** < **T3-N** < **T5-O** < **T1-N**

Fig. 1. Five possible modes of the binding of thymine to MoCp$_2^{2+}$.

Table 1. Energy (E, a.u), relative energy (ΔE, kcal/mol), dipole moment (μ, Debye), Electronic spatial extent (‹R$^2\rho$(R)›, a.u) and hydration energy ($\Delta E_{hydratiom}$, kcal/mol) values of various interaction modes of thymine and MoCp$_2^{2+}$ in gas and aqueous phases.

Molecule	gas					Aqueous			
	E	DE	‹R$^2\rho$(R)›	m		E	DE	DE$_{hydration}$	m
T1-N	-908.9444	15.42	4556.87	2.79		-909.1912	18.33	-154.89	3.38
T2-O	-908.9594	6.04	6487.46	5.17		-909.2159	2.85	-160.99	9.04
T3-N	-908.9366	20.35	5089.85	3.65		-909.1898	19.22	-158.94	5.65
T4-C	-908.9009	42.70	4152.65	5.56		-909.1627	36.22	-164.28	8.09
T5-O	-908.9690	0.00	5790.43	2.81		-909.2205	0.00	-157.80	4.21

3.2 Polarity

Calculated dipole moment values of the thymine and $MoCp_2Cl_2$ molecules are 4.21 and 7.24 Debye in gas phase, respectively. These values are 5.64 and 11.80 Debye in aqueous phase, thymine and $MoCp_2Cl_2$ molecules, respectively. Dipole moment values of five possible modes of the binding of thymine to $MoCp_2^{2+}$ are gathered in Table 1 for gas and aqueous phases. It can be deduced, larger polarity in **T2-O**, **T3-N** and **T4-C** isomers in compared to thymine. In contrast, polarities of **T1-N** and **T5-O** isomers are smaller in compared to thymine. On the other hand, polarities of all isomers are reduced in compared to $MoCp_2Cl_2$ complex.

It can be see, polarities of these molecules increase in aqueous phase than gas phase (Figure 2). Largest polarities are belonging to **T4-C** and **T2-O** isomers in gas and aqueous phases, respectively. Smallest polarity is belonging to **T1-N** isomer in gas and aqueous phases.
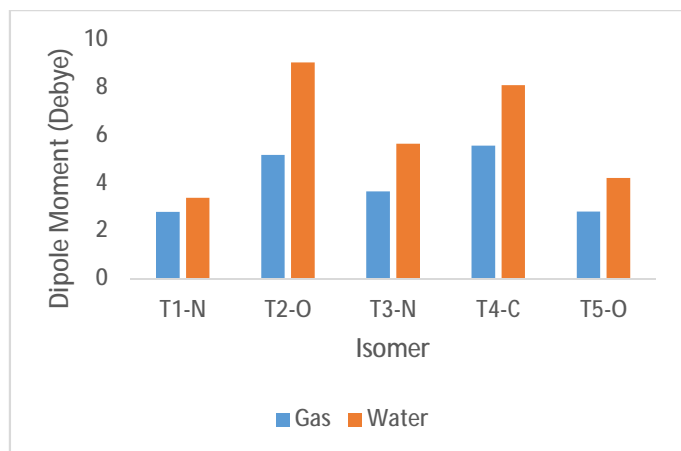

Fig. 2. Diagram of changing of dipole moment values of five possible modes of the binding of thymine to $MoCp_2^{2+}$ for gas and aqueous phase.

3.3 Electronic spatial extent (ESE)

Electronic spatial extent ($\langle R^2\rho(R)\rangle$) is descriptor of the molecule size. ESE is evaluated as multiplication of the anticipation value of the electron density and the distance from the center of molecule mass. In addition, it is typical physical property of the electron density volume around the molecule. Defusing of electron clod increases with increasing of the extent value. Computed ESE of thymine molecule is 1125.81 a.u. computed ESE values of five possible modes of the binding of thymine to $MoCp_2^{2+}$ are included in Table 1 for gas phase. It can be found, larger ESE values after binding of thymine to $MoCp_2^{2+}$.

3.4 Energy decomposition analysis (EDA)

To clarify the nature of the interaction of thymine and $MoCp_2$ complex, energy decomposition analysis (EDA) was used. The computed interaction energy data of the complexes in Table 2 are gathered. It can be observed most significance interaction occurs in **T1-N**-isomer. Computed polarization and steric energy (ΔE_{polar} and ΔE_{steric}) values are given in Table 2. The negative polarization energy values of stabilize thymine… $MoCp_2$ complex. However, the positive values of steric energy (sum of the exchanging and electrostatic energies) destabilize **T2-O**, **T3-N**, **T4-C** and **T5-O** complexes. The positive value of ΔE_{steric} stabilizes **T1-N** complex.

Table 2. EDA results of various interaction modes of thymine and $MoCp_2$ in gas phase (in kcal/mol).

Molecule	DE$_{int}$	DE$_{polar}$	DE$_{steric}$
T1-N	-94.66	-92.55	-2.10
T2-O	-86.87	-91.29	4.42
T3-N	-84.59	-91.58	6.99
T4-C	-66.75	-109.27	42.52
T5-O	-92.73	-99.27	6.54

3.5 Bond distances

In **T1-N** isomer, Mo-N and Mo-O bond lengths are 233.19 and 216.95 pm, respectively. In **T2-O** isomer, Mo-O bond distance is 199.00 pm. In **T3-N** isomer, Mo-N and Mo-C bond lengths are 236.76 and 217.68 pm, respectively. In **T4-C** isomer, Mo-C bond distance is 233.31 pm. In **T5-O** isomer, Mo-O bond distance is 197.05 pm. Shorter Mo-N bond of **T1-N** isomer than **T3-N** isomer is compatible with significance interaction between $MoCp_2$ and thymine in the basis of EDA results. Shorter Mo-O bond of **T5-O** isomer than **T2-O** isomer is well-matched with more effective interaction between $MoCp_2$ and thymine in the basis of EDA consequences.

3.6 Molecular Orbital analysis

Figure 3 illustrates the plots of frontier orbitals for the studied systems. In **T1-N** isomer, $MoCp_2$ fragment includes significance contribution in HOMO than thymine fragment. Reverse trend is shown for LUMO. In **T2-O** isomer, thymine fragment includes significance contribution in HOMO than $MoCp_2$ fragment. Converse tendency is exposed for LUMO. In **T4-C** isomer, $MoCp_2$ fragment includes significance contribution in HOMO than thymine fragment. Two fragment reveal more contribution in LUMO. In **T5-O** isomer, $MoCp_2$ fragment includes larger contribution in HOMO and LUMO than thymine fragment.

Table 3 shows the frontier orbital energy, HOMO-LUMO gap, hardness, chemical potential and

electrophilicity values in the investigated systems. It can be seen, frontier molecular orbitals of the Cp$_2$Mo…thymine complexes are more stabilize in compared to thymine. Also, there are smaller HOMO-LUMO gap and hardness values in the Cp$_2$Mo…thymine complexes than thymine.

Chemical potential values decrease in the Cp$_2$Mo…thymine complexes than thymine. In contrast, larger electrophilicity values are observed in the Cp$_2$Mo…thymine complexes than thymine.

Table 3. Frontier orbital energy. HOMO-LUMO gasp, hardness (η), chemical potential (μ) and electrophilicity (ω) values of various interaction modes of thymine and MoCp$_2{}^{2+}$ in gas phase ((ω,in eV).

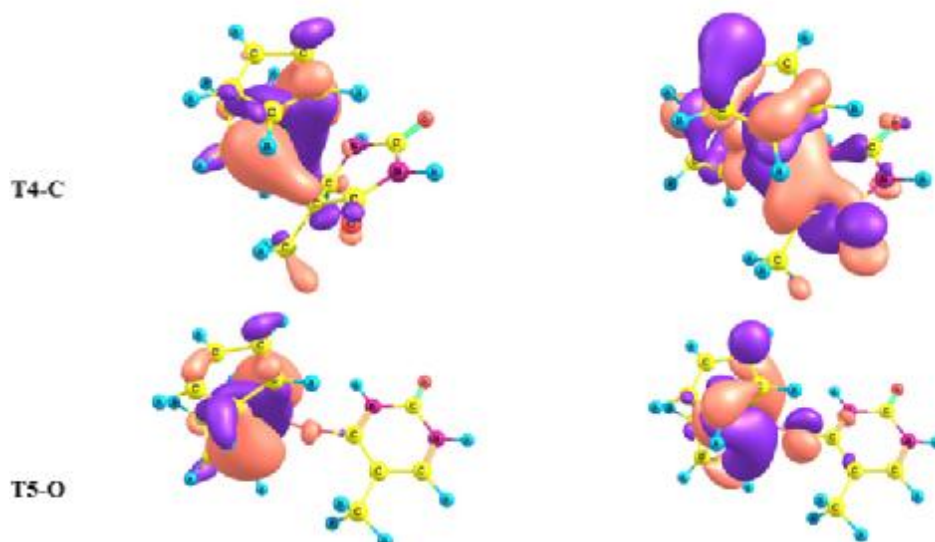| Molecule	E(HOMO)	E(LUMO)	Gap	h	m	w
Thymine	-7.03	-1.05	5.98	2.99	-4.04	2.73
T1-N	-13.69	-9.83	3.86	1.93	-11.76	35.86
T2-O	-13.67	-10.57	3.11	1.55	-12.12	47.26
T3-N	-13.91	-9.82	4.10	2.05	-11.86	34.36
T4-C	-14.26	-10.34	3.92	1.96	-12.30	38.60
T5-O	-13.61	-10.35	3.26	1.63	-11.98	43.97
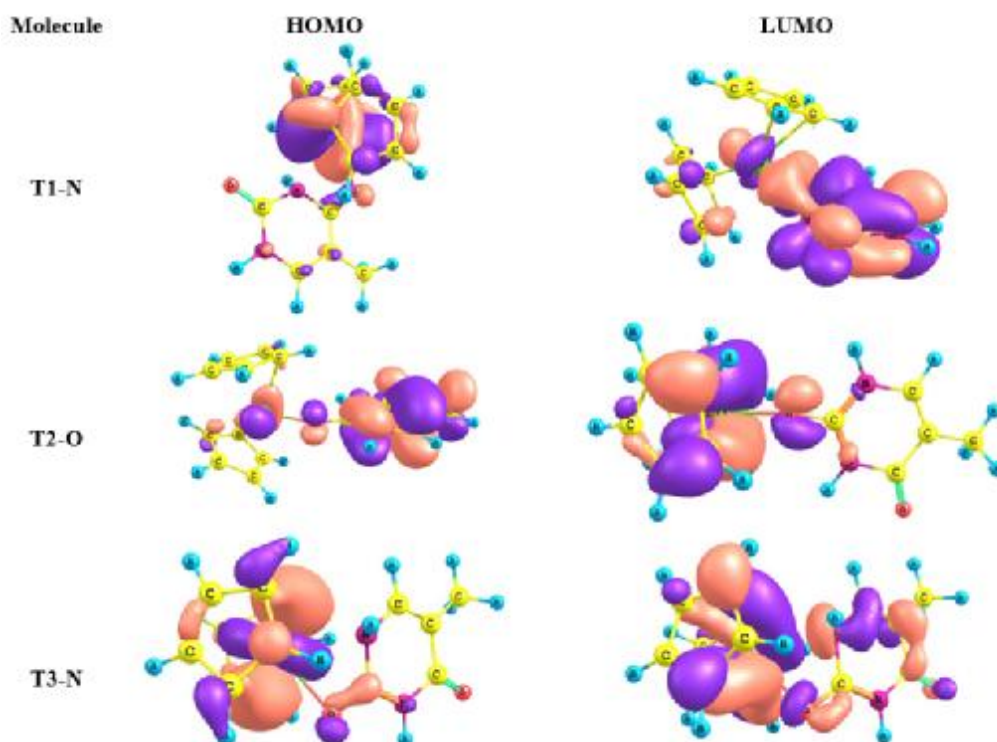
Figure 3. Frontier orbital plots of five possible modes of the binding of thymine to $MoCp_2^{2+}$.

3.7 Charge decomposition analysis (CDA)

The theory of charge decomposition analysis (CDA) is useful methods to provide a better understanding of the electron transfer. CDA results of the thymine … $MoCp_2$ complexes are provided. CDA results show that orbitals 47 of T1-N, 62 of T2-O, 48 of T3-N, 72 of T4-C and 65 of T5-O lead 0.04123, 0.05459, 0.03375, 0.03216 and 0.04327 electrons donate from thymine to $MoCp_2$, respectively. It can be deduced, the most electron donation is occurred in T2-O isomer.

3.8 QTAIM

QTAIM computations are used to illustration of the bond critical points (BCP) of thymine…$MoCp_2$ complexes.

Two bond critical points are identified between thymine and $MoCp_2$ in T1-N isomer: BCP(Mo-N) and BCP(Mo-O). ρ_{BCP}(Mo-N) and ρ_{BCP}(Mo-O) values of T1-N isomer are 5.90×10^{-2} and 7.87×10^{-2} e.Å^{-3}, respectively. $\nabla^2\rho_{BCP}$(Mo-N) and $\nabla^2\rho_{BCP}$(Mo-O) values of this isomer are 1.95×10^{-1} and 3.00×10^{-1} e.Å^{-5}, respectively. These positive interactions are compatible with the Mo-N and Mo-O bonds closed-shell interactions. Density of total electron energy (H) at BCP(Mo-N) and also BCP(Mo-O) of this isomer are -8.89×10^{-3} and -1.28×10^{-3}, e^2.Å^{-4}, respectively. The negative H values are considered as a covalency indicator [39]. The negative H values and positive $\nabla^2\rho$ values of BCP(Mo-N) and BCP(Mo-O) are compatible with similar systems [40, 41]. These values are compatible with a combination of the closed-shell and shared interactions for the Mo-N and Mo-O bonds.

One bond critical point is indicated between thymine and $MoCp_2$ in T2-O isomer: BCP(Mo-O). ρ_{BCP}(Mo-O),

$\nabla^2\rho_{BCP}$(Mo-O) and H(Mo-O) values are 1.11×10^{-1} e.Å^{-3}, 4.99×10^{-1} e.Å^{-5} and -2.92×10^{-2}, e^2.Å^{-4}, respectively. Again, negative H values and positive $\nabla^2\rho$ values reveal that mixture of the closed-shell and shared interactions for the Mo-O bond.

Two bond critical points are identified between thymine and $MoCp_2$ in T3-N isomer: BCP(Mo-N) and BCP(Mo-O). ρ_{BCP}(Mo-N) and ρ_{BCP}(Mo-O) values of this isomer are 5.54×10^{-2} and 7.76×10^{-2} e.Å^{-3}, respectively. $\nabla^2\rho_{BCP}$(Mo-N) and $\nabla^2\rho_{BCP}$(Mo-O) values of this isomer are 1.78×10^{-1} and 2.98×10^{-1} e.Å^{-5}, respectively. These positive interactions are compatible with the Mo-N and Mo-O bonds closed-shell interactions. Density of total electron energy (H) at BCP(Mo-N) and also BCP(Mo-O) of this isomer are -7.70×10^{-3} and -1.17×10^{-2}, e^2.Å^{-4}, respectively. Again, negative H values and positive $\nabla^2\rho$ values of BCP(Mo-N) and BCP(Mo-O) are compatible with combination of the closed-shell and shared interactions for the Mo-N and Mo-O bonds.

Two bond critical points are identified between thymine and $MoCp_2$ in T4-N isomer: BCP(Mo-C) and BCP(Mo-N). ρ_{BCP}(Mo-C) and ρ_{BCP}(Mo-N) values of this isomer are 6.66×10^{-2} and 6.25×10^{-2} e.Å^{-3}, respectively. $\nabla^2\rho_{BCP}$(Mo-C) and $\nabla^2\rho_{BCP}$(Mo-N) values of T4-N isomer are 1.30×10^{-1} and 2.31×10^{-1} e.Å^{-5}, respectively. These positive interactions are compatible with the Mo-C and Mo-N bonds closed-shell interactions. Density of total electron energy (H) at BCP(Mo-C) and also BCP(Mo-N) of this isomer are -1.84×10^{-2} and -8.83×10^{-3}, e^2.Å^{-4}, respectively. Again, negative H values and positive $\nabla^2\rho$ values of BCP(Mo-C) and BCP(Mo-N) are compatible with combination of the closed-shell and shared interactions for the Mo-C and Mo-N bonds.

One bond critical point is indicated between thymine and $MoCp_2$ in T5-O isomer: BCP(Mo-O). ρ_{BCP}(Mo-O), $\nabla^2\rho_{BCP}$(Mo-O) and H(Mo-O) values are 3.32×10^{-1} e.Å^{-3}, -1.49×10^{-1} e.Å^{-5} and -5.09×10^{-1}, e^2.Å^{-4}, respectively. Negative H and $\nabla^2\rho$ values reveal shared interactions for the Mo-O bond.

3.9 Interaction region indicator (IRI)

IRI is extremely useful in revealing all kinds of interaction regions of chemical system. IRI graphs of the investigated systems are presented in Figure 4. The graphical effect of the IRI map is obviously quite satisfactory. The weak interaction regions are exhibited nicely. The interaction region marked by green circle can be identified as vdW interaction region, which shows that the electron density in this region is low. The chemical bond regions are also clearly revealed by blue isosurfaces, indicating that electron density in these regions is very large and implying bonding effect is strong. Steric effect exists within the rings because the color of corresponding isosurfaces is red.
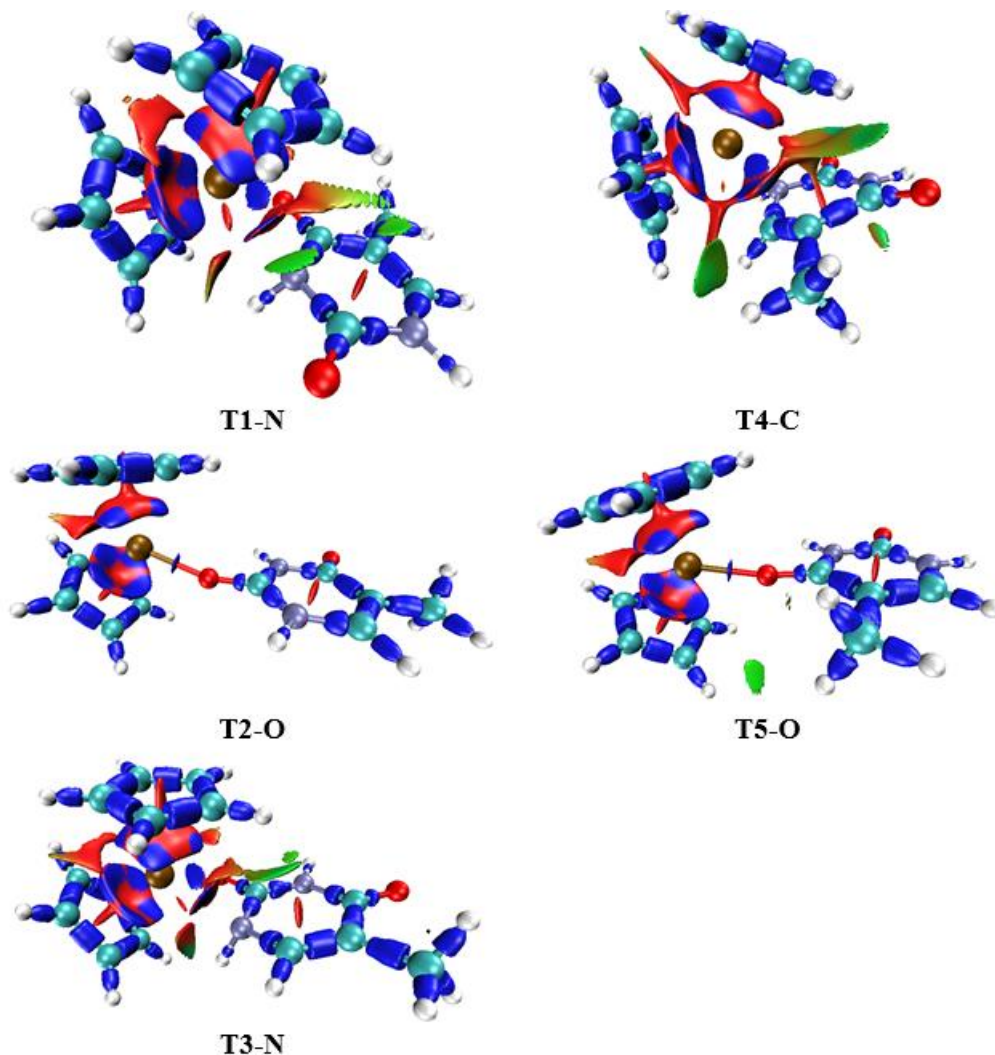

Figure 4. IRI graphs of five possible modes of the binding of thymine to $MoCp_2^{2+}$.

4. Conclusion:

Computational investigation of thymine with $MoCp_2^{2+}$ indicated the stability trend of these interactions was as: T5-O > T2-O > T1-N > T3-N > T4-C. EDA results revealed most significance interaction for in T1-N isomer. Polarity of **T2-O**, **T3-N** and **T4-C** isomers increased than thymine. In contrast, polarity of **T1-N** and **T5-O** isomers were smaller in compared to thymine. Largest polarities were belonged to **T4-C** and **T2-O** isomers in gas and aqueous phases, respectively. Smallest polarity was belonged to **T1-N** isomer in gas and aqueous phases. ESE values increased after binding of thymine to $MoCp_2^{2+}$. CDA consequences showed the most electron donation of thymine to $MoCp_2$ in T2-O isomer. QTAIM

computations illustrated mixture of the shared and closed-shell interactions for Mo-O and also Mo-N bonds in the studied systems. IRI graphs were revealed all kinds of interaction regions in the studied molecules.

References

[1] M.M. Harding, G. Mokdsi, Antitumour metallocenes: structure-activity studies and interactions with biomolecules *Curr. Med. Chem.*, 7 (2000) 1289.

[2] E. Mele´ndez, Titanium complexes in cancer treatment *Crit. Rev. Oncol. Hematol*, 42 (2002) 309.

[3] W. Kandioller, M. Reikersdorfer, S. Theiner, A. Roller, M. Hejl, M. A.Jakupec, M. S.Malarek, B. K.Keppler, The Impact of Leaving Group Variation on the Anticancer Activity of Molybdenocenes *Organometallics*, 37 (2018) 3909.

[4] H. Vinklárekb, Bioinorganic chemistry of vanadocene dichloride *Inorganica Chimica Acta*, 437 (2015) 87.

[5] R.P. Eberle, Y. Hari, S. Schürch, Specific Interactions of Antitumor Metallocenes with Deoxydinucleoside Monophosphates *J. Am. Soc. Mass Spectrom.*, 28 (2017) 1901.

[6] L.A. Profitt, R.H.G. Baxter, A.M. Valentine, Superstoichiometric Binding of the Anticancer Agent Titanocene Dichloride by Human Serum Transferrin and the Accompanying Lobe Closure *Biochemistry*, 61 (2022) 795.

[7] D. Sanna, V. Ugone, G. Micera, T. Pivetta, E. Valletta, E. Garribba, Speciation of the Potential Antitumor Agent Vanadocene Dichloride in the Blood Plasma and Model Systems *Inorg. Chem.* , 54 (2015) 8237.

[8] S.E. Johnson, T.A. Bell, J.K. West, Cp2TiCl2: Synthesis, Characterization, Modeling and Catalysis *J. Chem. Educ.*, (2022) 2121.

[9] M.G. Harriss, M.L.H. Green, W.E. Lindsell, Studies of bis-π-cyclopentadienyl-molybdenum and -tungsten complexes containing sulphur- and oxygen-bonded ligands *J. Chem. Soc. (A)*, (1969) 1453.

[10] E. Gore, M.L.H. Green, M.G. Harriss, W.E. Lindsell, H. Shaw, Some bis-π-cyclopentadienyl complexes of molybdenum and tungsten with sulphur, nitrogen, and oxygen ligands *J. Chem. Soc. (A)*, (1969) 1981.

[11] M.J. Calhorda, M.A.A.F.d.C.T. Carrondo, M.H. Garcia, M.B. Hursthouse, The X-ray crystal structure of di-η^5-cyclopentadienylthiophenolatoamminemolybdenum(IV) hexafluorophosphate solvate [Mo(η^5-C$_5$H$_5$)$_2$(NH$_3$)(SC$_6$H5)][PF$_6$] · (CH$_3$)$_2$CO *J. Organomet. Chem*, 342 (1988) 209.

[12] M. Domínguez, J.E. Cortés-Figueroa, E. Meléndez, Biological Interaction of Molybdenocene Dichloride with Bovine Serum Albumin Using Fluorescence Spectroscopy *J. Chem. Educ.*, 98 (2018) 152.

[13] M. Monajjemi, R. Ghiasi, M.A. Seyed Sadjadi, Metal-stabilized rare tautomers: N4 metalated cytosine (M = Li$^+$, Na$^+$, K$^+$, Rb+ and Cs$^+$), theoretical views *Applied Organometallic Chemistry*, 17 (2003) 635.

[14] R. Ghiasi, M. Monajjem, F. Asadian, H. Passdar, Theoretical investigation of the interaction of uracil and mono hydrated uracil - water complexes with alkali metals *Journal of Chemical Research*, (2004) 445.

[15] M. Monajjemi, R. Ghiasi, S. Ketabi, H. Passdar, F. Mollaamin, A theoretical study of metal-stabilised rare tautomers stability: N4 metalated cytosine (M=Be^{2+}, Mg^{2+}, Ca^{2+}, Sr $^{2+}$, and Ba^{2+}) in gas phase and different solvents *Journal of Chemical Research*, (2004) 11.

[16] M. Kamel, K. Mohammadifard, Thermodynamic and reactivity descriptors Studies on the interaction of Flutamide anticancer drug with nucleobases: A computational view *Chemical Review and Letters*, 4 (2021) 54.

[17] M. Rezaei-Sameti, Z.I. Borojeni, Interaction of 5-fluorouracil anticancer drug with nucleobases: insight from DFT, TD-DFT, and AIM calculations *Journal of Biomolecular Structure and Dynamics*, 41 (2023) 5882.

[18] S. Bilge, B. Dogan-Topal, T.T. Tok, E.B. Atici, A. Sınağ, S.A. Ozkan, Investigation of the interaction between anticancer drug ibrutinib and double-stranded DNA by electrochemical and molecular docking techniques *Microchemical Journal*, 180 (2022) 107622.

[19] R.P. Eberle, S. Schürch, Titanocene binding to oligonucleotides *J Inorg Biochem*, 184 (2018) 1.

[20] J. Karges, S.M. Cohen, Rhenium(V) Complexes as Cysteine-Targeting Coordinate Covalent Warheads *J. Med. Chem.*, 66 (2023) 3088.

[21] Z. Huang, J.J. Wilson, Therapeutic and Diagnostic Applications of Multimetallic Rhenium(I) Tricarbonyl Complexes *Eur. J. Inorg. Chem.*, (2021) 1312.

[22] E.J. Anthony, E.M. Bolitho, H.E. Bridgewater, O.W.L. Carter, J.M. Donnelly, C. Imberti, E.C. Lant, F. Lermyte, R.J. Needham, M. Palau, P.J. Sadler, H. Shi, F.-X. Wang, W.-Y. Zhang, Z. Zhang, Metallodrugs are unique: opportunities and challenges of discovery and development *Chem. Sci.*, 11 (2020) 12888.

[23] L.Y. Kuo, M.G. Kanatzidis, M. Sabat, A.L. Tipton, T.J. Marks, Metallocene antitumor agents. Solution and solid-state molybdenocene coordination chemistry of DNA constituents *J. Am. Chem. Soc.*, 113 (1991) 9027.

[24] M.J. Frisch, G.W. Trucks, H.B. Schlegel, G.E. Scuseria, M.A. Robb, J.R. Cheeseman, G. Scalmani, V. Barone, B. Mennucci, G.A. Petersson, H. Nakatsuji, M. Caricato, X. Li, H.P. Hratchian, A.F. Izmaylov, J. Bloino, G. Zheng, J.L. Sonnenberg, M. Hada, M. Ehara, K. Toyota, R. Fukuda, J. Hasegawa, M. Ishida, T. Nakajima, Y. Honda, O. Kitao, H. Nakai, T. Vreven, J. J. A. Montgomery, J.E. Peralta, F. Ogliaro, M. Bearpark, J.J. Heyd, E. Brothers, K.N. Kudin, V.N. Staroverov, T. Keith, R. Kobayashi, J. Normand, K. Raghavachari, A. Rendell, J.C. Burant, S.S. Iyengar, J. Tomasi, M. Cossi, N. Rega, J.M. Millam, M. Klene, J.E. Knox, J.B. Cross, V. Bakken, C. Adamo, J. Jaramillo, R. Gomperts, R.E. Stratmann, O. Yazyev, A.J. Austin, R. Cammi, C. Pomelli, J.W. Ochterski, R.L. Martin, K. Morokuma, V.G. Zakrzewski, G.A. Voth, P. Salvador, J.J. Dannenberg, S. Dapprich, A.D. Daniels, O.

Farkas, J.B. Foresman, J.V. Ortiz, J. Cioslowski, D.J. Fox, in, Gaussian, Inc., Wallingford CT, 2013.

[25] P.J. Hay, basis sets for molecular calculations - representation of 3D orbitals in transition-metal atoms *J. Chem. Phys.*, 66 (1977) 4377.

[26] R. Krishnan, J.S. Binkley, R. Seeger, J.A. Pople, self consistent molecular orbital methods. XX. A basis set for correlated wave functions *J. Chem. Phys.*, 72 (1980) 650.

[27] A.D. McLean, G.S. Chandler, Contracted Gaussian-basis sets for molecular calculations. 1. 2nd row atoms, Z=11-18 *J. Chem. Phys.*, 72 (1980) 5639.

[28] A.J.H. Wachters, Gaussian basis set for molecular wavefunctions containing third-row atoms *J. Chem. Phys.*, 52 (1970) 1033.

[29] D. Rappoport, F. Furche, Property-optimized Gaussian basis sets for molecular response calculations *J. Chem. Phys.*, 133 (2010) 134105

[30] D. Andrae, U. Haeussermann, M.Dolg, H.Stoll, H.Preuss, Energy-adjustedab initio pseudopotentials for the second and third row transition elements *Theor.Chim.Acta*, 77 (1990) 123.

[31] C. Adamo, V. Barone, Exchange functionals with improved long-range behavior and adiabatic connection methods without adjustable parameters: The mPW and mPW1PW models *J. Chem. Phys.* , 108 (1998) 664.

[32] V. Barone, M. Cossi, Quantum calculation of molecular energies and energy gradients in solution by a conductor solvent model *J. Phys. Chem. A*, 102 (1998) 1995.

[33] M. Cossi, N. Rega, G. Scalmani, V. Barone, Energies, structures, and electronic properties of molecules in solution with the C-PCM solvation model *J. Comp. Chem.*, 24 (2003) 669.

[34] T. Lu, F. Chen, Multiwfn: A Multifunctional Wavefunction Analyzer *J. Comp. Chem.*, 33 (2012) 580.

[35] T. Lu, Q. Chen, Interaction Region Indicator: A Simple Real Space Function Clearly Revealing Both Chemical Bonds and Weak Interactions *Chemistry—Methods*, 1 (2021) 231.

[36] M. Xiao, T. Lu, Generalized Charge Decomposition Analysis (GCDA) Method *Journal of Advances in Physical Chemistry*, 4 (2015) 111.

[37] T. Lu, F. Chen, Quantitative molecular surface analysis module: *J. Mol. Graph. Model*, 38 (2012) 314.

[38] W. Humphrey, A. Dalke, K. Schulten, VMD-Visual Molecular Dynamics *J. Mol. Graphics*, 14 (1996) 33.

[39] D. Cremer, E. Kraka, A description of the chemical-bond in terms of local properties of electron-density and energy *Croat. Chem. Acta*, 57 (1984) 1259.

[40] M. Palusiak, Substituent effect in para substituted $Cr(CO)_5$–pyridine complexes *J. Organometallic. Chem*, 692 (2005) 3866.

[41] P. Macchi, A. Sironi, Chemical bonding in transition metal carbonyl clusters: complementary analysis of theoretical and experimental electron densities. *Coordination Chemistry Reviews* 239 (2003) 383.